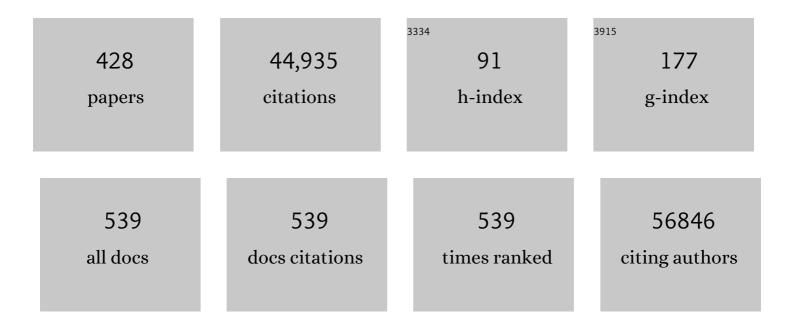
List of Publications by Year in descending order

Source: https://exaly.com/author-pdf/3553837/publications.pdf Version: 2024-02-01



FARIAN | THEIS

#	Article	IF	CITATIONS
1	Mapping single-cell data to reference atlases by transfer learning. Nature Biotechnology, 2022, 40, 121-130.	17.5	236
2	Cell-Type-Specific Impact of Glucocorticoid Receptor Activation on the Developing Brain: A Cerebral Organoid Study. American Journal of Psychiatry, 2022, 179, 375-387.	7.2	33
3	Toward modeling metabolic state from single-cell transcriptomics. Molecular Metabolism, 2022, 57, 101396.	6.5	27
4	Integration of single-cell transcriptomes and chromatin landscapes reveals regulatory programs driving pharyngeal organ development. Nature Communications, 2022, 13, 457.	12.8	22
5	Squidpy: a scalable framework for spatial omics analysis. Nature Methods, 2022, 19, 171-178.	19.0	308
6	CellRank for directed single-cell fate mapping. Nature Methods, 2022, 19, 159-170.	19.0	286
7	The discovAIR project: a roadmap towards the Human Lung Cell Atlas. European Respiratory Journal, 2022, 60, 2102057.	6.7	15
8	Effect of Atmospheric Aging on Soot Particle Toxicity in Lung Cell Models at the Air–Liquid Interface: Differential Toxicological Impacts of Biogenic and Anthropogenic Secondary Organic Aerosols (SOAs). Environmental Health Perspectives, 2022, 130, 27003.	6.0	44
9	Spatial components of molecular tissue biology. Nature Biotechnology, 2022, 40, 308-318.	17.5	148
10	A Python library for probabilistic analysis of single-cell omics data. Nature Biotechnology, 2022, 40, 163-166.	17.5	216
11	Benchmarking atlas-level data integration in single-cell genomics. Nature Methods, 2022, 19, 41-50.	19.0	403
12	Ultraâ€high sensitivity mass spectrometry quantifies singleâ€cell proteome changes upon perturbation. Molecular Systems Biology, 2022, 18, e10798.	7.2	261
13	Parkinson's disease motor symptoms rescue by CRISPRaâ€reprogramming astrocytes into GABAergic neurons. EMBO Molecular Medicine, 2022, 14, e14797.	6.9	26
14	Mature neutrophils and a NFkB-to-IFN transition determine the unifying disease recovery dynamics in COVID-19. Cell Reports Medicine, 2022, , 100652.	6.5	9
15	Ketamine exerts its sustained antidepressant effects via cell-type-specific regulation of Kcnq2. Neuron, 2022, 110, 2283-2298.e9.	8.1	40
16	Ly6D+Siglec-H+ precursors contribute to conventional dendritic cells via a Zbtb46+Ly6D+ intermediary stage. Nature Communications, 2022, 13, .	12.8	7
17	Exposure to naphthalene and β-pinene-derived secondary organic aerosol induced divergent changes in transcript levels of BEAS-2B cells. Environment International, 2022, 166, 107366.	10.0	18
18	Heterogeneous Development of β-Cell Populations in Diabetes-Resistant and -Susceptible Mice. Diabetes, 2022, 71, 1962-1978.	0.6	3

#	Article	IF	CITATIONS
19	Asthma in farm children is more determined by genetic polymorphisms and in nonâ€farm children by environmental factors. Pediatric Allergy and Immunology, 2021, 32, 295-304.	2.6	17
20	CD23 Levels on B Cells Determine Long-Term Therapeutic Response in Patients with Atopic Eczema Treated with Selective IgE Immune Apheresis. Journal of Investigative Dermatology, 2021, 141, 681-685.e6.	0.7	1
21	Non-canonical Wnt/PCP signalling regulates intestinal stem cell lineage priming towards enteroendocrine and Paneth cell fates. Nature Cell Biology, 2021, 23, 23-31.	10.3	46
22	Single-cell molecular profiling of all three components of the HPA axis reveals adrenal ABCB1 as a regulator of stress adaptation. Science Advances, 2021, 7, .	10.3	42
23	Deep learning the collisional cross sections of the peptide universe from a million experimental values. Nature Communications, 2021, 12, 1185.	12.8	81
24	Deep Learning-based Propensity Scores for Confounding Control in Comparative Effectiveness Research. Epidemiology, 2021, 32, 378-388.	2.7	15
25	Asc-1 regulates white versus beige adipocyte fate in a subcutaneous stromal cell population. Nature Communications, 2021, 12, 1588.	12.8	17
26	Posterior subcapsular cataracts are a late effect after acute exposure to 0.5 Gy ionizing radiation in mice. International Journal of Radiation Biology, 2021, 97, 529-540.	1.8	5
27	Integrated intra―and intercellular signaling knowledge for multicellular omics analysis. Molecular Systems Biology, 2021, 17, e9923.	7.2	152
28	Integrative analysis of cell state changes in lung fibrosis with peripheral protein biomarkers. EMBO Molecular Medicine, 2021, 13, e12871.	6.9	53
29	Comparison of genome-wide gene expression profiling by RNA Sequencing <i>versus</i> microarray in bronchial biopsies of COPD patients before and after inhaled corticosteroid treatment: does it provide new insights?. ERJ Open Research, 2021, 7, 00104-2021.	2.6	2
30	Graph representation learning for single-cell biology. Current Opinion in Systems Biology, 2021, 28, 100347.	2.6	15
31	Swarm Learning for decentralized and confidential clinical machine learning. Nature, 2021, 594, 265-270.	27.8	375
32	Cellular connectomes as arbiters of local circuit models in the cerebral cortex. Nature Communications, 2021, 12, 2785.	12.8	11
33	Epithelial cell plasticity drives endoderm formation during gastrulation. Nature Cell Biology, 2021, 23, 692-703.	10.3	41
34	Machine learning for perturbational single-cell omics. Cell Systems, 2021, 12, 522-537.	6.2	52
35	Single-cell RNA sequencing reveals ex vivo signatures of SARS-CoV-2-reactive T cells through â€~reverse phenotyping'. Nature Communications, 2021, 12, 4515.	12.8	23
36	AutoGeneS: Automatic gene selection using multi-objective optimization for RNA-seq deconvolution. Cell Systems, 2021, 12, 706-715.e4.	6.2	44

#	Article	IF	CITATIONS
37	CD81 marks immature and dedifferentiated pancreatic β-cells. Molecular Metabolism, 2021, 49, 101188.	6.5	26
38	Sfaira accelerates data and model reuse in single cell genomics. Genome Biology, 2021, 22, 248.	8.8	18
39	Group Testing for SARS-CoV-2 Allows for Up to 10-Fold Efficiency Increase Across Realistic Scenarios and Testing Strategies. Frontiers in Public Health, 2021, 9, 583377.	2.7	25
40	RNA velocity—current challenges and future perspectives. Molecular Systems Biology, 2021, 17, e10282.	7.2	130
41	Early IFN-α signatures and persistent dysfunction are distinguishing features of NK cells in severe COVID-19. Immunity, 2021, 54, 2650-2669.e14.	14.3	145
42	EpiScanpy: integrated single-cell epigenomic analysis. Nature Communications, 2021, 12, 5228.	12.8	59
43	Diet-induced alteration of intestinal stem cell function underlies obesity and prediabetes in mice. Nature Metabolism, 2021, 3, 1202-1216.	11.9	47
44	Current Smoking Alters Gene Expression and DNA Methylation in the Nasal Epithelium of Patients with Asthma. American Journal of Respiratory Cell and Molecular Biology, 2021, 65, 366-377.	2.9	10
45	Vertical sleeve gastrectomy triggers fast β-cell recovery upon overt diabetes. Molecular Metabolism, 2021, 54, 101330.	6.5	10
46	Identification and characterization of distinct brown adipocyte subtypes in C57BL/6J mice. Life Science Alliance, 2021, 4, e202000924.	2.8	14
47	A field guide to cultivating computational biology. PLoS Biology, 2021, 19, e3001419.	5.6	6
48	Over 1000 tools reveal trends in the single-cell RNA-seq analysis landscape. Genome Biology, 2021, 22, 301.	8.8	85
49	scCODA is a Bayesian model for compositional single-cell data analysis. Nature Communications, 2021, 12, 6876.	12.8	98
50	SARS-CoV-2 infection triggers profibrotic macrophage responses and lung fibrosis. Cell, 2021, 184, 6243-6261.e27.	28.9	277
51	scPower accelerates and optimizes the design of multi-sample single cell transcriptomic studies. Nature Communications, 2021, 12, 6625.	12.8	38
52	Impact of Brain Fatty Acid Signaling on Peripheral Insulin Action in Mice. Experimental and Clinical Endocrinology and Diabetes, 2020, 128, 20-29.	1.2	2
53	Altered relaxation times in MRI indicate bronchopulmonary dysplasia. Thorax, 2020, 75, 184-187.	5.6	22
54	ILâ€17C amplifies epithelial inflammation in human psoriasis and atopic eczema. Journal of the European Academy of Dermatology and Venereology, 2020, 34, 800-809.	2.4	26

#	Article	IF	CITATIONS
55	Alveolar regeneration through a Krt8+ transitional stem cell state that persists in human lung fibrosis. Nature Communications, 2020, 11, 3559.	12.8	378
56	LifeTime and improving European healthcare through cell-based interceptive medicine. Nature, 2020, 587, 377-386.	27.8	108
57	Severe COVID-19 Is Marked by a Dysregulated Myeloid Cell Compartment. Cell, 2020, 182, 1419-1440.e23.	28.9	1,162
58	Generalizing RNA velocity to transient cell states through dynamical modeling. Nature Biotechnology, 2020, 38, 1408-1414.	17.5	1,460
59	<i>In vivo</i> identification of apoptotic and extracellular vesicleâ€bound live cells using imageâ€based deep learning. Journal of Extracellular Vesicles, 2020, 9, 1792683.	12.2	18
60	Self-supervised retinal thickness prediction enables deep learning from unlabelled data to boost classification of diabetic retinopathy. Nature Machine Intelligence, 2020, 2, 719-726.	16.0	48
61	Predicting single-cell gene expression profiles of imaging flow cytometry data with machine learning. Nucleic Acids Research, 2020, 48, 11335-11346.	14.5	16
62	Inhibition of LTβR signalling activates WNT-induced regeneration in lung. Nature, 2020, 588, 151-156.	27.8	81
63	Post-surgical adhesions are triggered by calcium-dependent membrane bridges between mesothelial surfaces. Nature Communications, 2020, 11, 3068.	12.8	42
64	The proteome landscape of the kingdoms of life. Nature, 2020, 582, 592-596.	27.8	128
65	Automatic identification of relevant genes from low-dimensional embeddings of single-cell RNA-seq data. Bioinformatics, 2020, 36, 4291-4295.	4.1	7
66	Model-based analysis of response and resistance factors of cetuximab treatment in gastric cancer cell lines. PLoS Computational Biology, 2020, 16, e1007147.	3.2	8
67	Protocol of a population-based prospective COVID-19 cohort study Munich, Germany (KoCo19). BMC Public Health, 2020, 20, 1036.	2.9	42
68	DeepWAS: Multivariate genotype-phenotype associations by directly integrating regulatory information using deep learning. PLoS Computational Biology, 2020, 16, e1007616.	3.2	54
69	Eleven grand challenges in single-cell data science. Genome Biology, 2020, 21, 31.	8.8	742
70	Targeted pharmacological therapy restores β-cell function for diabetes remission. Nature Metabolism, 2020, 2, 192-209.	11.9	93
71	Epithelial Planar Bipolarity Emerges from Notch-Mediated Asymmetric Inhibition of Emx2. Current Biology, 2020, 30, 1142-1151.e6.	3.9	25
72	SARS-CoV-2 Receptor ACE2 Is an Interferon-Stimulated Gene in Human Airway Epithelial Cells and Is Detected in Specific Cell Subsets across Tissues. Cell, 2020, 181, 1016-1035.e19.	28.9	1,956

#	Article	IF	CITATIONS
73	A sparse deep learning approach for automatic segmentation of human vasculature in multispectral optoacoustic tomography. Photoacoustics, 2020, 20, 100203.	7.8	26
74	Conditional out-of-distribution generation for unpaired data using transfer VAE. Bioinformatics, 2020, 36, i610-i617.	4.1	62
75	Predicting antigen specificity of single T cells basedÂon <scp>TCR CDR</scp> 3 regions. Molecular Systems Biology, 2020, 16, e9416.	7.2	68
76	The single-cell eQTLGen consortium. ELife, 2020, 9, .	6.0	150
77	Is the humoral immunity dispensable for the pathogenesis of psoriasis?. Journal of the European Academy of Dermatology and Venereology, 2019, 33, 115-122.	2.4	10
78	BART-Seq: cost-effective massively parallelized targeted sequencing for genomics, transcriptomics, and single-cell analysis. Genome Biology, 2019, 20, 155.	8.8	19
79	scGen predicts single-cell perturbation responses. Nature Methods, 2019, 16, 715-721.	19.0	290
80	Evaluation of Deep Learning Strategies for Nucleus Segmentation in Fluorescence Images. Cytometry Part A: the Journal of the International Society for Analytical Cytology, 2019, 95, 952-965.	1.5	205
81	scSLAM-seq reveals core features of transcription dynamics in single cells. Nature, 2019, 571, 419-423.	27.8	153
82	Meeting the Challenges of High-Dimensional Single-Cell Data Analysis in Immunology. Frontiers in Immunology, 2019, 10, 1515.	4.8	67
83	GENOTYPE, PRENATAL ENVIRONMENT OR BOTH–WHAT SHAPES THE NEWBORN'S EPIGENOME?. European Neuropsychopharmacology, 2019, 29, S1036-S1037.	0.7	0
84	Concepts and limitations for learning developmental trajectories from single cell genomics. Development (Cambridge), 2019, 146, .	2.5	177
85	F96POLYGENIC RISK SCORE ANALYSIS OF TRAJECTORIES OF COGNITIVE PERFORMANCE IN PSYCHIATRIC PATIENTS. European Neuropsychopharmacology, 2019, 29, S1161.	0.7	0
86	Pheno-seq – linking visual features and gene expression in 3D cell culture systems. Scientific Reports, 2019, 9, 12367.	3.3	16
87	Current best practices in singleâ€cell RNAâ€seq analysis: a tutorial. Molecular Systems Biology, 2019, 15, e8746.	7.2	1,322
88	MPRAnalyze: statistical framework for massively parallel reporter assays. Genome Biology, 2019, 20, 183.	8.8	58
89	A map of β-cell differentiation pathways supports cell therapies for diabetes. Nature, 2019, 569, 342-343.	27.8	8
90	Establishment of a high-resolution 3D modeling system for studying pancreatic epithelial cell biology inÂvitro. Molecular Metabolism, 2019, 30, 16-29.	6.5	22

#	Article	IF	CITATIONS
91	Aldh1b1 expression defines progenitor cells in the adult pancreas and is required for Kras-induced pancreatic cancer. Proceedings of the National Academy of Sciences of the United States of America, 2019, 116, 20679-20688.	7.1	41
92	Single-cell RNA-seq denoising using a deep count autoencoder. Nature Communications, 2019, 10, 390.	12.8	668
93	IRE11±-XBP1s pathway promotes prostate cancer by activating c-MYC signaling. Nature Communications, 2019, 10, 323.	12.8	158
94	Dynamic modelling of an ACADS genotype in fatty acid oxidation – Application of cellular models for the analysis of common genetic variants. PLoS ONE, 2019, 14, e0216110.	2.5	1
95	A cellular census of human lungs identifies novel cell states in health and in asthma. Nature Medicine, 2019, 25, 1153-1163.	30.7	631
96	Inferring Interaction Networks From Multi-Omics Data. Frontiers in Genetics, 2019, 10, 535.	2.3	105
97	Massive single-cell mRNA profiling reveals a detailed roadmap for pancreatic endocrinogenesis. Development (Cambridge), 2019, 146, .	2.5	145
98	Integrated analysis of environmental and genetic influences on cord blood DNA methylation in new-borns. Nature Communications, 2019, 10, 2548.	12.8	94
99	PAGA: graph abstraction reconciles clustering with trajectory inference through a topology preserving map of single cells. Genome Biology, 2019, 20, 59.	8.8	911
100	Common patterns of gene regulation associated with Cesarean section and the development of islet autoimmunity – indications of immune cell activation. Scientific Reports, 2019, 9, 6250.	3.3	4
101	The Human Lung Cell Atlas: A High-Resolution Reference Map of the Human Lung in Health and Disease. American Journal of Respiratory Cell and Molecular Biology, 2019, 61, 31-41.	2.9	178
102	Deep learning: new computational modelling techniques for genomics. Nature Reviews Genetics, 2019, 20, 389-403.	16.3	717
103	Inferring population dynamics from single-cell RNA-sequencing time series data. Nature Biotechnology, 2019, 37, 461-468.	17.5	85
104	A strategy for highâ€dimensional multivariable analysis classifies childhood asthma phenotypes from genetic, immunological, and environmental factors. Allergy: European Journal of Allergy and Clinical Immunology, 2019, 74, 1364-1373.	5.7	24
105	An atlas of the aging lung mapped by single cell transcriptomics and deep tissue proteomics. Nature Communications, 2019, 10, 963.	12.8	408
106	SA125POLYGENIC BURDEN ANALYSIS OF LONGITUDINAL CLUSTERS OF PSYCHOPATHOLOGICAL FEATURES IN A CROSS-DIAGNOSTIC GROUP OF INDIVIDUALS WITH SEVERE MENTAL ILLNESS. European Neuropsychopharmacology, 2019, 29, S1257-S1258.	0.7	0
107	Editorial: Integrative Computational Systems Biology Approaches in Immunology and Medicine. Frontiers in Microbiology, 2019, 9, 3338.	3.5	1
108	A test metric for assessing single-cell RNA-seq batch correction. Nature Methods, 2019, 16, 43-49.	19.0	278

#	Article	IF	CITATIONS
109	Metabolic regulation of pluripotency and germ cell fate through αâ€ketoglutarate. EMBO Journal, 2019, 38, .	7.8	77
110	Whither systems medicine?. Experimental and Molecular Medicine, 2018, 50, e453-e453.	7.7	49
111	Cell type atlas and lineage tree of a whole complex animal by single-cell transcriptomics. Science, 2018, 360, .	12.6	381
112	<i>netReg</i> : network-regularized linear models for biological association studies. Bioinformatics, 2018, 34, 896-898.	4.1	12
113	Maternal whole blood cell miRNA-340 is elevated in gestational diabetes and inversely regulated by glucose and insulin. Scientific Reports, 2018, 8, 1366.	3.3	38
114	Epigenetically Regulated Chromosome 14q32 miRNA Cluster Induces Metastasis and Predicts Poor Prognosis in Lung Adenocarcinoma Patients. Molecular Cancer Research, 2018, 16, 390-402.	3.4	63
115	Lifetime study in mice after acute low-dose ionizing radiation: a multifactorial study with special focus on cataract risk. Radiation and Environmental Biophysics, 2018, 57, 99-113.	1.4	30
116	Type I Immune Response Induces Keratinocyte Necroptosis and Is Associated with Interface Dermatitis. Journal of Investigative Dermatology, 2018, 138, 1785-1794.	0.7	52
117	Dynamic landscape of pancreatic carcinogenesis reveals early molecular networks of malignancy. Gut, 2018, 67, 146-156.	12.1	43
118	Prediction of type 1 diabetes using a genetic risk model in the Diabetes Autoimmunity Study in the Young. Pediatric Diabetes, 2018, 19, 277-283.	2.9	19
119	Early Identification of Bronchopulmonary Dysplasia Using Novel Biomarkers by Proteomic Screening. American Journal of Respiratory and Critical Care Medicine, 2018, 197, 1076-1080.	5.6	26
120	Toll-like receptor 7/8 agonists stimulate plasmacytoid dendritic cells to initiate TH17-deviated acute contact dermatitis in human subjects. Journal of Allergy and Clinical Immunology, 2018, 141, 1320-1333.e11.	2.9	44
121	MicroRNA as an Integral Part of Cell Communication: Regularized Target Prediction and Network Prediction. Lecture Notes in Bioengineering, 2018, , 85-100.	0.4	0
122	Information Theoretic Concepts to Unravel Cell–Cell Communication. Lecture Notes in Bioengineering, 2018, , 115-136.	0.4	0
123	Mechanistic description of spatial processes using integrative modelling of noise-corrupted imaging data. Journal of the Royal Society Interface, 2018, 15, 20180600.	3.4	2
124	Efficient Parameter Estimation Enables the Prediction of Drug Response Using a Mechanistic Pan-Cancer Pathway Model. Cell Systems, 2018, 7, 567-579.e6.	6.2	99
125	Characterization of missing values in untargeted MS-based metabolomics data and evaluation of missing data handling strategies. Metabolomics, 2018, 14, 128.	3.0	138
126	Multi-experiment nonlinear mixed effect modeling of single-cell translation kinetics after transfection. Npj Systems Biology and Applications, 2018, 4, 1.	3.0	66

#	Article	IF	CITATIONS
127	Increasing Neural Stem Cell Division Asymmetry and Quiescence Are Predicted to Contribute to the Age-Related Decline in Neurogenesis. Cell Reports, 2018, 25, 3231-3240.e8.	6.4	35
128	Copy number aberrations from Affymetrix SNP 6.0 genotyping data—how accurate are commonly used prediction approaches?. Briefings in Bioinformatics, 2018, , .	6.5	3
129	Bayesian parameter estimation for biochemical reaction networks using region-based adaptive parallel tempering. Bioinformatics, 2018, 34, i494-i501.	4.1	14
130	LNA++: Linear Noise Approximation with First and Second Order Sensitivities. Lecture Notes in Computer Science, 2018, , 300-306.	1.3	0
131	Inductive and Selective Effects of GSK3 and MEK Inhibition on Nanog Heterogeneity in Embryonic Stem Cells. Stem Cell Reports, 2018, 11, 58-69.	4.8	25
132	Lineage marker synchrony in hematopoietic genealogies refutes the PU.1/GATA1 toggle switch paradigm. Nature Communications, 2018, 9, 2697.	12.8	24
133	SCANPY: large-scale single-cell gene expression data analysis. Genome Biology, 2018, 19, 15.	8.8	3,958
134	Impulse model-based differential expression analysis of time course sequencing data. Nucleic Acids Research, 2018, 46, e119.	14.5	81
135	MetaMap: an atlas of metatranscriptomic reads in human disease-related RNA-seq data. GigaScience, 2018, 7, .	6.4	22
136	Data Driven Computational Modeling of Hematopoiesis in Myelodysplastic Syndromes Unveils Differences in Hematopoietic Stem Cell Kinetics Compared to Age-Matched Healthy Controls. Blood, 2018, 132, 4354-4354.	1.4	0
137	Parameter estimation for dynamical systems with discrete events and logical operations. Bioinformatics, 2017, 33, 1049-1056.	4.1	36
138	Inhibition of fat cell differentiation in 3T3-L1 pre-adipocytes by all-trans retinoic acid: Integrative analysis of transcriptomic and phenotypic data. Biomolecular Detection and Quantification, 2017, 11, 31-44.	7.0	9
139	Parallelization and High-Performance Computing Enables Automated Statistical Inference of Multi-scale Models. Cell Systems, 2017, 4, 194-206.e9.	6.2	62
140	AURKA, DLGAP5, TPX2, KIF11 and CKAP5: Five specific mitosis-associated genes correlate with poor prognosis for non-small cell lung cancer patients. International Journal of Oncology, 2017, 50, 365-372.	3.3	110
141	cgCorrect: a method to correct for confounding cell–cell variation due to cell growth in single-cell transcriptomics. Physical Biology, 2017, 14, 036001.	1.8	15
142	Prospective identification of hematopoietic lineage choice by deep learning. Nature Methods, 2017, 14, 403-406.	19.0	160
143	Pulmonary microRNA profiles identify involvement of Creb1 and Sec14l3 in bronchial epithelial changes in allergic asthma. Scientific Reports, 2017, 7, 46026.	3.3	29
144	fastER: a user-friendly tool for ultrafast and robust cell segmentation in large-scale microscopy. Bioinformatics, 2017, 33, 2020-2028.	4.1	58

#	Article	IF	CITATIONS
145	Identification of a plasma mi <scp>RNA</scp> biomarker signature for allergic asthma: A translational approach. Allergy: European Journal of Allergy and Clinical Immunology, 2017, 72, 1962-1971.	5.7	51
146	Model-based branching point detection in single-cell data by K-branches clustering. Bioinformatics, 2017, 33, 3211-3219.	4.1	13
147	A BaSiC tool for background and shading correction of optical microscopy images. Nature Communications, 2017, 8, 14836.	12.8	213
148	Label Free Identification of Peripheral Blood Eosinophils Using High-Throughput Imaging Flow Cytometry. Journal of Allergy and Clinical Immunology, 2017, 139, AB163.	2.9	0
149	GATA2/3-TFAP2A/C transcription factor network couples human pluripotent stem cell differentiation to trophectoderm with repression of pluripotency. Proceedings of the National Academy of Sciences of the United States of America, 2017, 114, E9579-E9588.	7.1	130
150	Integrating Polygenic Allele Burden Information And Phenomic Data To Characterize Complex Disease Trajectories In Severe Mental Illness. European Neuropsychopharmacology, 2017, 27, S406.	0.7	0
151	POLYGENIC BURDEN ANALYSIS OF LONGITUDINAL CLUSTERS OF QUALITY OF LIFE AND FUNCTIONING IN PATIENTS WITH SEVERE MENTAL ILLNESS. European Neuropsychopharmacology, 2017, 27, S408-S409.	0.7	0
152	The Role Of Micrornas In The Course Of Severe Mental Disorders. European Neuropsychopharmacology, 2017, 27, S456-S457.	0.7	0
153	Reconstructing cell cycle and disease progression using deep learning. Nature Communications, 2017, 8, 463.	12.8	210
154	Single cells make big data: New challenges and opportunities in transcriptomics. Current Opinion in Systems Biology, 2017, 4, 85-91.	2.6	171
155	Systematic single-cell analysis provides new insights into heterogeneity and plasticity of the pancreas. Molecular Metabolism, 2017, 6, 974-990.	6.5	95
156	Network inference from glycoproteomics data reveals new reactions in the IgG glycosylation pathway. Nature Communications, 2017, 8, 1483.	12.8	67
157	Comprehensive benchmarking of Markov chain Monte Carlo methods for dynamical systems. BMC Systems Biology, 2017, 11, 63.	3.0	34
158	Peptide serum markers in islet autoantibody-positive children. Diabetologia, 2017, 60, 287-295.	6.3	24
159	TALEN/CRISPR-mediated engineering of a promoterless anti-viral RNAi hairpin into an endogenous miRNA locus. Nucleic Acids Research, 2017, 45, e3-e3.	14.5	8
160	pulver: an R package for parallel ultra-rapid p-value computation for linear regression interaction terms. BMC Bioinformatics, 2017, 18, 429.	2.6	1
161	A scalable moment-closure approximation for large-scale biochemical reaction networks. Bioinformatics, 2017, 33, i293-i300.	4.1	2
162	Model Based Targeting of IL-6-Induced Inflammatory Responses in Cultured Primary Hepatocytes to Improve Application of the JAK Inhibitor Ruxolitinib. Frontiers in Physiology, 2017, 8, 775.	2.8	19

#	Article	IF	CITATIONS
163	The Human Cell Atlas. ELife, 2017, 6, .	6.0	1,547
164	Correcting Classifiers for Sample Selection Bias in Two-Phase Case-Control Studies. Computational and Mathematical Methods in Medicine, 2017, 2017, 1-18.	1.3	8
165	Scalable Parameter Estimation for Genome-Scale Biochemical Reaction Networks. PLoS Computational Biology, 2017, 13, e1005331.	3.2	125
166	Calcium-regulatory proteins as modulators of chemotherapy in human neuroblastoma. Oncotarget, 2017, 8, 22876-22893.	1.8	27
167	2D cross-omics integrated enrichment analysis reveals insights into COPD pathogenesis. , 2017, , .		0
168	CERENA: ChEmical REaction Network Analyzer—A Toolbox for the Simulation and Analysis of Stochastic Chemical Kinetics. PLoS ONE, 2016, 11, e0146732.	2.5	35
169	A novel molecular disease classifier for psoriasis and eczema. Experimental Dermatology, 2016, 25, 767-774.	2.9	54
170	Software tools for single-cell tracking and quantification of cellular and molecular properties. Nature Biotechnology, 2016, 34, 703-706.	17.5	162
171	Separation of Uncorrelated Stationary time series using Autocovariance Matrices. Journal of Time Series Analysis, 2016, 37, 337-354.	1.2	36
172	Quantitative comparison of competing PDE models for Pomlp dynamics in fission yeast * *The authors acknowledge financial support from the Postdoctoral Fellowship Program (PFP) of the Helmholtz Zentrum Munchen IFAC-PapersOnLine, 2016, 49, 264-269.	0.9	2
173	Metabolomics reveals effects of maternal smoking on endogenous metabolites from lipid metabolism in cord blood of newborns. Metabolomics, 2016, 12, 76.	3.0	18
174	Computational approaches for systems metabolomics. Current Opinion in Biotechnology, 2016, 39, 198-206.	6.6	53
175	Editorial overview: Systems biology-the intersection of experiments and computation, underpinning biotechnology. Current Opinion in Biotechnology, 2016, 39, iv-vi.	6.6	0
176	Metabolomics screening identifies reduced <scp>L</scp> -carnitine to be associated with progressive emphysema. Clinical Science, 2016, 130, 273-287.	4.3	39
177	Diffusion pseudotime robustly reconstructs lineage branching. Nature Methods, 2016, 13, 845-848.	19.0	982
178	Analysis of Cell Lineage Trees by Exact Bayesian Inference Identifies Negative Autoregulation of Nanog in Mouse Embryonic Stem Cells. Cell Systems, 2016, 3, 480-490.e13.	6.2	30
179	Lactation is associated with altered metabolomic signatures in women with gestational diabetes. Diabetologia, 2016, 59, 2193-2202.	6.3	20
180	Early myeloid lineage choice is not initiated by random PU.1 to GATA1 protein ratios. Nature, 2016, 535, 299-302.	27.8	180

#	Article	IF	CITATIONS
181	Tailored parameter optimization methods for ordinary differential equation models with steady-state constraints. BMC Systems Biology, 2016, 10, 80.	3.0	30
182	MEMO: multi-experiment mixture model analysis of censored data. Bioinformatics, 2016, 32, 2464-2472.	4.1	7
183	A computational model to predict severity of atopic eczema from 30 serum proteins. Journal of Allergy and Clinical Immunology, 2016, 138, 1207-1210.e2.	2.9	13
184	A subset of metastatic pancreatic ductal adenocarcinomas depends quantitatively on oncogenic Kras/Mek/Erk-induced hyperactive mTOR signalling. Gut, 2016, 65, 647-657.	12.1	57
185	The global gene expression profile of the secondary transition during pancreatic development. Mechanisms of Development, 2016, 139, 51-64.	1.7	32
186	<i>destiny</i> : diffusion maps for large-scale single-cell data in R. Bioinformatics, 2016, 32, 1241-1243.	4.1	518
187	Combinatorial Histone Acetylation Patterns Are Generated by Motif-Specific Reactions. Cell Systems, 2016, 2, 49-58.	6.2	19
188	Unbiased Prediction and Feature Selection in High-Dimensional Survival Regression. Journal of Computational Biology, 2016, 23, 279-290.	1.6	21
189	Epigenetic germline inheritance of diet-induced obesity and insulin resistance. Nature Genetics, 2016, 48, 497-499.	21.4	287
190	Label-free cell cycle analysis for high-throughput imaging flow cytometry. Nature Communications, 2016, 7, 10256.	12.8	237
191	Interleukin-4 and interferon-Î ³ orchestrate an epithelial polarization in the airways. Mucosal Immunology, 2016, 9, 917-926.	6.0	81
192	An adaptive scheduling scheme for calculating Bayes factors with thermodynamic integration using Simpson's rule. Statistics and Computing, 2016, 26, 663-677.	1.5	15
193	Inferring catalysis in biological systems. IET Systems Biology, 2016, 10, 210-218.	1.5	1
194	Inference for Stochastic Chemical Kinetics Using Moment Equations and System Size Expansion. PLoS Computational Biology, 2016, 12, e1005030.	3.2	77
195	Pitchfork and Gprasp2 Target Smoothened to the Primary Cilium for Hedgehog Pathway Activation. PLoS ONE, 2016, 11, e0149477.	2.5	21
196	miTALOS v2: Analyzing Tissue Specific microRNA Function. PLoS ONE, 2016, 11, e0151771.	2.5	60
197	MicroRNA-138 promotes acquired alkylator resistance in glioblastoma by targeting the Bcl-2-interacting mediator BIM. Oncotarget, 2016, 7, 12937-12950.	1.8	58
198	Mitosis Detection in Intestinal Crypt Images with Hough Forest and Conditional Random Fields. Lecture Notes in Computer Science, 2016, , 287-295.	1.3	0

#	Article	IF	CITATIONS
199	Abstract 1945: Identification of a miRNA/mRNA network driving non-small cell lung cancer (NSCLC) dissemination. , 2016, , .		0
200	LSC Abstract – Systemic and local metabolomics profiling reveals novel insights into the progression of emphysema. , 2016, , .		0
201	LSC Abstract – Early biomarkers indicating the development of neonatal chronic lung disease defined by clinical and imaging parameters. , 2016, , .		Ο
202	LSC Abstract – Systemic and local metabolomics profiling reveals novel insights into the progression of emphysema. , 2016, , .		0
203	Atrx promotes heterochromatin formation atÂretrotransposons. EMBO Reports, 2015, 16, 836-850.	4.5	126
204	Inference of spatiotemporal effects on cellular state transitions from time-lapse microscopy. BMC Systems Biology, 2015, 9, 61.	3.0	3
205	MicroRNA-Target Network Inference and Local Network Enrichment Analysis Identify Two microRNA Clusters with Distinct Functions in Head and Neck Squamous Cell Carcinoma. International Journal of Molecular Sciences, 2015, 16, 30204-30222.	4.1	12
206	Integrative Analysis of MicroRNA and mRNA Data Reveals an Orchestrated Function of MicroRNAs in Skeletal Myocyte Differentiation in Response to TNF-α or IGF1. PLoS ONE, 2015, 10, e0135284.	2.5	21
207	Diffusion maps for high-dimensional single-cell analysis of differentiation data. Bioinformatics, 2015, 31, 2989-2998.	4.1	576
208	Opposing effects of allogrooming on disease transmission in ant societies. Philosophical Transactions of the Royal Society B: Biological Sciences, 2015, 370, 20140108.	4.0	43
209	Combined Single-Cell Functional and Gene Expression Analysis Resolves Heterogeneity within Stem Cell Populations. Cell Stem Cell, 2015, 16, 712-724.	11.1	376
210	Quantification of regenerative potential in primary human mammary epithelial cells. Development (Cambridge), 2015, 142, 3239-51.	2.5	105
211	Gender-specific pathway differences in the human serum metabolome. Metabolomics, 2015, 11, 1815-1833.	3.0	218
212	Anatomic-landmark detection using graphical context modelling. , 2015, , .		1
213	Decoding the regulatory network of early blood development from single-cell gene expression measurements. Nature Biotechnology, 2015, 33, 269-276.	17.5	352
214	Model selection using limiting distributions of second-order blind source separation algorithms. Signal Processing, 2015, 113, 95-103.	3.7	27
215	Computational analysis of cell-to-cell heterogeneity in single-cell RNA-sequencing data reveals hidden subpopulations of cells. Nature Biotechnology, 2015, 33, 155-160.	17.5	1,068
216	Fast clonal expansion and limited neural stem cell self-renewal in the adult subependymal zone. Nature Neuroscience, 2015, 18, 490-492.	14.8	160

#	Article	IF	CITATIONS
217	Identifying latent dynamic components in biological systems. IET Systems Biology, 2015, 9, 193-203.	1.5	5
218	Transcriptional Mechanisms of Proneural Factors and REST in Regulating Neuronal Reprogramming of Astrocytes. Cell Stem Cell, 2015, 17, 74-88.	11.1	187
219	Multi-omic signature of body weight change: results from a population-based cohort study. BMC Medicine, 2015, 13, 48.	5.5	69
220	Metabolism gene signatures and surgical site infections in abdominal surgery. International Journal of Surgery, 2015, 14, 67-74.	2.7	3
221	Live imaging of adult neural stem cell behavior in the intact and injured zebrafish brain. Science, 2015, 348, 789-793.	12.6	156
222	Next-generation sequencing reveals novel differentially regulated mRNAs, lncRNAs, miRNAs, sdRNAs and a piRNA in pancreatic cancer. Molecular Cancer, 2015, 14, 94.	19.2	210
223	Network plasticity of pluripotency transcription factors in embryonic stem cells. Nature Cell Biology, 2015, 17, 1235-1246.	10.3	130
224	Stem-Cell-like Properties and Epithelial Plasticity Arise as Stable Traits after Transient Twist1 Activation. Cell Reports, 2015, 10, 131-139.	6.4	155
225	SimiRa: A tool to identify coregulation between microRNAs and RNA-binding proteins. RNA Biology, 2015, 12, 998-1009.	3.1	14
226	Reconstructing gene regulatory dynamics from high-dimensional single-cell snapshot data. Bioinformatics, 2015, 31, i89-i96.	4.1	134
227	RAMONA: a Web application for gene set analysis on multilevel omics data. Bioinformatics, 2015, 31, 128-130.	4.1	7
228	Network-Based Approach for Analyzing Intra- and Interfluid Metabolite Associations in Human Blood, Urine, and Saliva. Journal of Proteome Research, 2015, 14, 1183-1194.	3.7	40
229	An Affine Equivariant Robust Second-Order BSS Method. Lecture Notes in Computer Science, 2015, , 328-335.	1.3	3
230	Approximate Bayesian Computation for Stochastic Single-Cell Time-Lapse Data Using Multivariate Test Statistics. Lecture Notes in Computer Science, 2015, , 52-63.	1.3	4
231	Data-Driven Modelling of Biological Multi-Scale Processes. Journal of Coupled Systems and Multiscale Dynamics, 2015, 3, 101-121.	0.2	37
232	The Human Blood Metabolome-Transcriptome Interface. PLoS Genetics, 2015, 11, e1005274.	3.5	99
233	A Critical Period for Postnatal Adaptive Plasticity in a Model of Motor Axon Miswiring. PLoS ONE, 2015, 10, e0123643.	2.5	6
234	Allergic Contact Dermatitis in Psoriasis Patients: Typical, Delayed, and Non-Interacting. PLoS ONE, 2014, 9, e101814.	2.5	30

#	Article	IF	CITATIONS
235	Proteome-wide analysis reveals an age-associated cellular phenotype of in situ aged human fibroblasts. Aging, 2014, 6, 856-872.	3.1	65
236	ODE Constrained Mixture Modelling: A Method for Unraveling Subpopulation Structures and Dynamics. PLoS Computational Biology, 2014, 10, e1003686.	3.2	44
237	Feature ranking of type 1 diabetes susceptibility genes improves prediction of type 1 diabetes. Diabetologia, 2014, 57, 2521-2529.	6.3	112
238	Uncertainty Analysis for Non-identifiable Dynamical Systems: Profile Likelihoods, Bootstrapping and More. Lecture Notes in Computer Science, 2014, , 61-72.	1.3	33
239	MCA: Multiresolution Correlation Analysis, a graphical tool for subpopulation identification in single-cell gene expression data. BMC Bioinformatics, 2014, 15, 240.	2.6	9
240	Intraindividual genome expression analysis reveals a specific molecular signature of psoriasis and eczema. Science Translational Medicine, 2014, 6, 244ra90.	12.4	170
241	Novel genetic associations with serum level metabolites identified by phenotype set enrichment analyses. Human Molecular Genetics, 2014, 23, 5847-5857.	2.9	26
242	Radial Basis Function Approximations of Bayesian Parameter Posterior Densities for Uncertainty Analysis. Lecture Notes in Computer Science, 2014, , 73-85.	1.3	4
243	Metabolite profiling reveals new insights into the regulation of serum urate in humans. Metabolomics, 2014, 10, 141-151.	3.0	51
244	A strategy to find gene combinations that identify children who progress rapidly to type 1 diabetes after islet autoantibody seroconversion. Acta Diabetologica, 2014, 51, 403-411.	2.5	20
245	Method of conditional moments (MCM) for the Chemical Master Equation. Journal of Mathematical Biology, 2014, 69, 687-735.	1.9	86
246	Probabilistic PCA of censored data: accounting for uncertainties in the visualization of high-throughput single-cell qPCR data. Bioinformatics, 2014, 30, 1867-1875.	4.1	21
247	An atlas of genetic influences on human blood metabolites. Nature Genetics, 2014, 46, 543-550.	21.4	1,084
248	Hypothalamic miR-103 Protects from Hyperphagic Obesity in Mice. Journal of Neuroscience, 2014, 34, 10659-10674.	3.6	76
249	Bayesian Blind Source Separation for Data with Network Structure. Journal of Computational Biology, 2014, 21, 855-865.	1.6	5
250	Cytokine-Regulated GADD45G Induces Differentiation and Lineage Selection in Hematopoietic Stem Cells. Stem Cell Reports, 2014, 3, 34-43.	4.8	40
251	Parameterizing cell-to-cell regulatory heterogeneities via stochastic transcriptional profiles. Proceedings of the National Academy of Sciences of the United States of America, 2014, 111, E626-35.	7.1	37
252	Decoding the transcriptional program for blood development from whole tissue single-cell gene expression measurements. Experimental Hematology, 2014, 42, S52.	0.4	0

#	Article	IF	CITATIONS
253	Cytokine-regulated GADD45G induces differentiation and lineage selection in hematopoietic stem cells. Experimental Hematology, 2014, 42, S57.	0.4	1
254	miR-335 promotes mesendodermal lineage segregation and shapes a transcription factor gradient in the endoderm. Development (Cambridge), 2014, 141, 514-525.	2.5	20
255	Mouse IDGenes: a reference database for genetic interactions in the developing mouse brain. Database: the Journal of Biological Databases and Curation, 2014, 2014, bau083-bau083.	3.0	2
256	Posttranscriptional Regulatory Networks: From Expression Profiling to Integrative Analysis of mRNA and MicroRNA Data. Methods in Molecular Biology, 2014, 1160, 165-188.	0.9	8
257	Centroid Clustering of Cellular Lineage Trees. Lecture Notes in Computer Science, 2014, , 15-29.	1.3	3
258	Effects of smoking and smoking cessation on human serum metabolite profile: results from the KORA cohort study. BMC Medicine, 2013, 11, 60.	5.5	103
259	Sharpening of expression domains induced by transcription and microRNA regulationwithin a spatio-temporal model of mid-hindbrain boundary formation. BMC Systems Biology, 2013, 7, 48.	3.0	16
260	Metabolomic profiles in individuals with negative affectivity and social inhibition: A population-based study of Type D personality. Psychoneuroendocrinology, 2013, 38, 1299-1309.	2.7	37
261	Myeloid lineage choice is not controlled by the PU.1 - Gata1 switch. Experimental Hematology, 2013, 41, S69.	0.4	0
262	An automatic method for robust and fast cell detection in bright field images from high-throughput microscopy. BMC Bioinformatics, 2013, 14, 297.	2.6	117
263	Modeling of 2D diffusion processes based on microscopy data: parameter estimation and practical identifiability analysis. BMC Bioinformatics, 2013, 14, S7.	2.6	15
264	Dependent component analysis. Eurasip Journal on Advances in Signal Processing, 2013, 2013, .	1.7	3
265	Visualizing edge-edge relations in graphs. , 2013, , .		4
266	Genome-wide association analyses identify 18 new loci associated with serum urate concentrations. Nature Genetics, 2013, 45, 145-154.	21.4	675
267	Extrinsically regulated Gadd45γ balances hematopoietic stem cell self-renewal and differentiation. Experimental Hematology, 2013, 41, S41.	0.4	0
268	Wound-healing growth factor, basic FGF, induces Erk1/2-dependent mechanical hyperalgesia. Pain, 2013, 154, 2216-2226.	4.2	41
269	The cytokine-induced microrna193b modulates ckit expression and STAT5 signaling. Experimental Hematology, 2013, 41, S45.	0.4	0
270	High-dimensional Bayesian parameter estimation: Case study for a model of JAK2/STAT5 signaling. Mathematical Biosciences, 2013, 246, 293-304.	1.9	56

#	Article	IF	CITATIONS
271	Integrative genetic and metabolite profiling analysis suggests altered phosphatidylcholine metabolism in asthma. Allergy: European Journal of Allergy and Clinical Immunology, 2013, 68, 629-636.	5.7	70
272	Characterization of transcriptional networks in blood stem and progenitor cells using high-throughput single-cell gene expression analysis. Nature Cell Biology, 2013, 15, 363-372.	10.3	257
273	Live imaging of astrocyte responses to acute injury reveals selective juxtavascular proliferation. Nature Neuroscience, 2013, 16, 580-586.	14.8	340
274	STATISTICAL METHODS FOR THE ANALYSIS OF HIGH-THROUGHPUT METABOLOMICS DATA. Computational and Structural Biotechnology Journal, 2013, 4, e201301009.	4.1	228
275	iVUN: interactive Visualization of Uncertain biochemical reaction Networks. BMC Bioinformatics, 2013, 14, S2.	2.6	11
276	A modular framework for gene set analysis integrating multilevel omics data. Nucleic Acids Research, 2013, 41, 9622-9633.	14.5	32
277	Truth-Content and Phase Transitions of Random Boolean Networks with Generic Logics. SIAM Journal on Applied Dynamical Systems, 2013, 12, 315-351.	1.6	1
278	The human transcriptome is enriched for miRNA-binding sites located in cooperativity-permitting distance. RNA Biology, 2013, 10, 1125-1135.	3.1	38
279	A Vine-copula Based Adaptive MCMC Sampler for Efficient Inference of Dynamical Systems. Bayesian Analysis, 2013, 8, .	3.0	17
280	Joining forces of Bayesian and frequentist methodology: a study for inference in the presence of non-identifiability. Philosophical Transactions Series A, Mathematical, Physical, and Engineering Sciences, 2013, 371, 20110544.	3.4	94
281	Lessons Learned from Quantitative Dynamical Modeling in Systems Biology. PLoS ONE, 2013, 8, e74335.	2.5	275
282	Social Transfer of Pathogenic Fungus Promotes Active Immunisation in Ant Colonies. PLoS Biology, 2012, 10, e1001300.	5.6	158
283	A novel approach for resolving differences in single-cell gene expression patterns from zygote to blastocyst. Bioinformatics, 2012, 28, i626-i632.	4.1	50
284	Specific temperature-induced perturbations of secondary mRNA structures are associated with the cold-adapted temperature-sensitive phenotype of influenza A virus. RNA Biology, 2012, 9, 1266-1274.	3.1	17
285	A Unilateral Negative Feedback Loop Between <i>miR-200</i> microRNAs and Sox2/E2F3 Controls Neural Progenitor Cell-Cycle Exit and Differentiation. Journal of Neuroscience, 2012, 32, 13292-13308.	3.6	98
286	Mining the Unknown: A Systems Approach to Metabolite Identification Combining Genetic and Metabolic Information. PLoS Genetics, 2012, 8, e1003005.	3.5	170
287	Systematic Complexity Reduction of Signaling Models and Application to a CD95 Signaling Model for Apoptosis. , 2012, , 57-84.		0
288	The dynamic range of the human metabolome revealed by challenges. FASEB Journal, 2012, 26, 2607-2619.	0.5	268

#	Article	IF	CITATIONS
289	Bayesian Independent Component Analysis Recovers Pathway Signatures from Blood Metabolomics Data. Journal of Proteome Research, 2012, 11, 4120-4131.	3.7	24
290	Identification and Quantification of 1-Hydroxybutene-2-yl Mercapturic Acid in Human Urine by UPLC- HILIC-MS/MS as a Novel Biomarker for 1,3-Butadiene Exposure. Chemical Research in Toxicology, 2012, 25, 1565-1567.	3.3	14
291	A strategy for combining minor genetic susceptibility genes to improve prediction of disease in type 1 diabetes. Genes and Immunity, 2012, 13, 549-555.	4.1	63
292	On the hypothesis-free testing of metabolite ratios in genome-wide and metabolome-wide association studies. BMC Bioinformatics, 2012, 13, 120.	2.6	121
293	Bayesian model selection validates a biokinetic model for zirconium processing in humans. BMC Systems Biology, 2012, 6, 95.	3.0	19
294	Stability and Multiattractor Dynamics of a Toggle Switch Based on a Two-Stage Model of Stochastic Gene Expression. Biophysical Journal, 2012, 102, 19-29.	0.5	76
295	Uniqueness of linear factorizations into independent subspaces. Journal of Multivariate Analysis, 2012, 112, 48-62.	1.0	5
296	Body Fat Free Mass Is Associated with the Serum Metabolite Profile in a Population-Based Study. PLoS ONE, 2012, 7, e40009.	2.5	95
297	The Sox17â€mCherry fusion mouse line allows visualization of endoderm and vascular endothelial development. Genesis, 2012, 50, 496-505.	1.6	37
298	Multiâ€scale modeling of GMP differentiation based on singleâ€cell genealogies. FEBS Journal, 2012, 279, 3488-3500.	4.7	19
299	ICA over finite fields—Separability and algorithms. Signal Processing, 2012, 92, 1796-1808.	3.7	33
300	The signal separation evaluation campaign (2007–2010): Achievements and remaining challenges. Signal Processing, 2012, 92, 1928-1936.	3.7	128
301	An Ensemble Approach for Inferring Semi-quantitative Regulatory Dynamics for the Differentiation of Mouse Embryonic Stem Cells Using Prior Knowledge. Advances in Experimental Medicine and Biology, 2012, 736, 247-260.	1.6	4
302	Systems Biology Meets Metabolism. , 2012, , 281-313.		1
303	PhenomiR: MicroRNAs in Human Diseases and Biological Processes. Methods in Molecular Biology, 2012, 822, 249-260.	0.9	57
304	Joint Diagonalization of Several Scatter Matrices for ICA. Lecture Notes in Computer Science, 2012, , 172-179.	1.3	3
305	Bayesian Fuzzy Clustering of Colored Graphs. Lecture Notes in Computer Science, 2012, , 528-535.	1.3	2
306	Bayesian Inference of Latent Causes in Gene Regulatory Dynamics. Lecture Notes in Computer Science, 2012, , 520-527.	1.3	0

#	Article	IF	CITATIONS
307	To Infinity and Beyond: On ICA over Hilbert Spaces. Lecture Notes in Computer Science, 2012, , 180-187.	1.3	0
308	Dynamic Mathematical Modeling of IL13-Induced Signaling in Hodgkin and Primary Mediastinal B-Cell Lymphoma Allows Prediction of Therapeutic Targets. Cancer Research, 2011, 71, 693-704.	0.9	82
309	Uniqueness of Non-Gaussianity-Based Dimension Reduction. IEEE Transactions on Signal Processing, 2011, 59, 4478-4482.	5.3	9
310	The Nature and Perception of Fluctuations in Human Musical Rhythms. PLoS ONE, 2011, 6, e26457.	2.5	63
311	Gaussian graphical modeling reveals specific lipid correlations in glioblastoma cells. Proceedings of SPIE, 2011, , .	0.8	1
312	The Heckscher–Ohlin model and the network structure of international trade. International Review of Economics and Finance, 2011, 20, 135-145.	4.5	44
313	Theoretical Analysis of Time-to-Peak Responses inÂBiological Reaction Networks. Bulletin of Mathematical Biology, 2011, 73, 978-1003.	1.9	4
314	Effective Parameters Determining the Information Flow in Hierarchical Biological Systems. Bulletin of Mathematical Biology, 2011, 73, 706-725.	1.9	5
315	MicroRNAs coordinately regulate protein complexes. BMC Systems Biology, 2011, 5, 136.	3.0	49
316	Gaussian graphical modeling reconstructs pathway reactions from high-throughput metabolomics data. BMC Systems Biology, 2011, 5, 21.	3.0	262
317	Steadyâ€state robustness of qualitative gene regulation networks. International Journal of Robust and Nonlinear Control, 2011, 21, 1742-1758.	3.7	6
318	Dynamic regimes of random fuzzy logic networks. New Journal of Physics, 2011, 13, 013041.	2.9	1
319	Vertex centralities in input-output networks reveal the structure of modern economies. Physical Review E, 2011, 83, 046127.	2.1	110
320	Huge Splicing Frequency in Human Y Chromosomal <i>UTY</i> Gene. OMICS A Journal of Integrative Biology, 2011, 15, 141-154.	2.0	11
321	MIPS: curated databases and comprehensive secondary data resources in 2010. Nucleic Acids Research, 2011, 39, D220-D224.	14.5	77
322	Complex Principal Component and Correlation Structure of 16 Yeast Genomic Variables. Molecular Biology and Evolution, 2011, 28, 2501-2512.	8.9	10
323	miTALOS: Analyzing the tissue-specific regulation of signaling pathways by human and mouse microRNAs. Rna, 2011, 17, 809-819.	3.5	52
324	Discovery of Sexual Dimorphisms in Metabolic and Genetic Biomarkers. PLoS Genetics, 2011, 7, e1002215.	3.5	328

#	Article	IF	CITATIONS
325	Hierarchical Differentiation of Myeloid Progenitors Is Encoded in the Transcription Factor Network. PLoS ONE, 2011, 6, e22649.	2.5	137
326	The <i>a</i> _{<i>d</i>} coefficient as a descriptive measure of the withinâ€group agreement of ratings. British Journal of Mathematical and Statistical Psychology, 2010, 63, 341-360.	1.4	6
327	Information-Theoretic Model Selection for Independent Components. Lecture Notes in Computer Science, 2010, , 254-262.	1.3	1
328	Odefy - From discrete to continuous models. BMC Bioinformatics, 2010, 11, 233.	2.6	102
329	Structuring heterogeneous biological information using fuzzy clustering of k-partite graphs. BMC Bioinformatics, 2010, 11, 522.	2.6	18
330	Knowledge-based matrix factorization temporally resolves the cellular responses to IL-6 stimulation. BMC Bioinformatics, 2010, 11, 585.	2.6	16
331	Intronic microRNAs support their host genes by mediating synergistic and antagonistic regulatory effects. BMC Genomics, 2010, 11, 224.	2.8	126
332	Biologically meaningful update rules increase the critical connectivity of generalized Kauffman networks. Journal of Theoretical Biology, 2010, 266, 436-448.	1.7	8
333	Tissue-Specific Target Analysis of Disease-Associated MicroRNAs in Human Signaling Pathways. PLoS ONE, 2010, 5, e11154.	2.5	16
334	The Structure of Borders in a Small World. PLoS ONE, 2010, 5, e15422.	2.5	122
335	From Binary to Multivalued to Continuous Models: The lac Operon as a Case Study. Journal of Integrative Bioinformatics, 2010, 7, .	1.5	8
336	MicroRNA Loss Enhances Learning and Memory in Mice. Journal of Neuroscience, 2010, 30, 14835-14842.	3.6	276
337	Patterns of Subnet Usage Reveal Distinct Scales of Regulation in the Transcriptional Regulatory Network of Escherichia coli. PLoS Computational Biology, 2010, 6, e1000836.	3.2	15
338	Colored Subspace Analysis: Dimension Reduction Based on a Signal's Autocorrelation Structure. IEEE Transactions on Circuits and Systems I: Regular Papers, 2010, 57, 1463-1474.	5.4	7
339	PhenomiR: a knowledgebase for microRNA expression in diseases and biological processes. Genome Biology, 2010, 11, R6.	9.6	247
340	The 2010 Signal Separation Evaluation Campaign (SiSEC2010): Audio Source Separation. Lecture Notes in Computer Science, 2010, , 114-122.	1.3	25
341	Second Order Subspace Analysis and Simple Decompositions. Lecture Notes in Computer Science, 2010, , 370-377.	1.3	4
342	Robust Second-Order Source Separation Identifies Experimental Responses in Biomedical Imaging. Lecture Notes in Computer Science, 2010, , 466-473.	1.3	5

#	Article	IF	CITATIONS
343	ICA over Finite Fields. Lecture Notes in Computer Science, 2010, , 645-652.	1.3	10
344	From binary to multivalued to continuous models: the lac operon as a case study. Journal of Integrative Bioinformatics, 2010, 7, .	1.5	8
345	The 2010 Signal Separation Evaluation Campaign (SiSEC2010): Biomedical Source Separation. Lecture Notes in Computer Science, 2010, , 123-130.	1.3	2
346	Second-Order Source Separation Based on Prior Knowledge Realized in a Graph Model. Lecture Notes in Computer Science, 2010, , 434-441.	1.3	10
347	Robust Stability Analysis and Design Under Consideration of Multiple Feedback Loops of the Tryptophan Regulatory Network of Escherichia coli. Advances in Experimental Medicine and Biology, 2010, 680, 189-197.	1.6	0
348	Hypergraphs and Cellular Networks. PLoS Computational Biology, 2009, 5, e1000385.	3.2	316
349	Spatial Analysis of Expression Patterns Predicts Genetic Interactions at the Mid-Hindbrain Boundary. PLoS Computational Biology, 2009, 5, e1000569.	3.2	36
350	Transforming Boolean models to continuous models: methodology and application to T-cell receptor signaling. BMC Systems Biology, 2009, 3, 98.	3.0	212
351	Reconstruction of graphs based on random walks. Theoretical Computer Science, 2009, 410, 3826-3838.	0.9	6
352	ICA, kernel methods and nonnegativity: New paradigms for dynamical component analysis of fMRI data. Engineering Applications of Artificial Intelligence, 2009, 22, 497-504.	8.1	10
353	Blind Source Separation Techniques for the Decomposition of Multiply Labeled Fluorescence Images. Biophysical Journal, 2009, 96, 3791-3800.	0.5	113
354	Blind Source Separation Techniques For The Decomposition Of Multiply Labeled Fluorescence Images. Biophysical Journal, 2009, 96, 32a.	0.5	3
355	Zebrafish reward mutants reveal novel transcripts mediating the behavioral effects of amphetamine. Genome Biology, 2009, 10, R81.	9.6	71
356	Soft Dimension Reduction for ICA by Joint Diagonalization on the Stiefel Manifold. Lecture Notes in Computer Science, 2009, , 354-361.	1.3	22
357	Estimating Hidden Influences in Metabolic and Gene Regulatory Networks. Lecture Notes in Computer Science, 2009, , 387-394.	1.3	2
358	Blind Decomposition of Spectral Imaging Microscopy: A Study on Artificial and Real Test Data. Lecture Notes in Computer Science, 2009, , 548-556.	1.3	6
359	Hierarchical Extraction of Independent Subspaces of Unknown Dimensions. Lecture Notes in Computer Science, 2009, , 259-266.	1.3	5
360	Analyzing M-CSF dependent monocyte/macrophage differentiation: Expression modes and meta-modes derived from an independent component analysis. BMC Bioinformatics, 2008, 9, 100.	2.6	20

3

#	ARTICLE	IF	CITATIONS
361	An evolutionary and structural characterization of mammalian protein complex organization. BMC Genomics, 2008, 9, 629.	2.8	20
362	A robust model for spatiotemporal dependencies. Neurocomputing, 2008, 71, 2209-2216.	5.9	10
363	Hybridizing sparse component analysis with genetic algorithms for microarray analysis. Neurocomputing, 2008, 71, 2356-2376.	5.9	14
364	Erythropoietin enhances hippocampal long-term potentiation and memory. BMC Biology, 2008, 6, 37.	3.8	129
365	Money Circulation, Trackable Items, and the Emergence of Universal Human Mobility Patterns. IEEE Pervasive Computing, 2008, 7, 28-35.	1.3	57
366	Knowledge-based gene expression classification via matrix factorization. Bioinformatics, 2008, 24, 1688-1697.	4.1	36
367	Gene regulatory networks simplified by nonlinear balanced truncation. , 2008, , .		5
368	Episode-Specific Differential Gene Expression of Peripheral Blood Mononuclear Cells in Rapid Cycling Supports Novel Treatment Approaches. Molecular Medicine, 2008, 14, 546-552.	4.4	25
369	Effective Emission Tomography Image Reconstruction Algorithms for SPECT Data. Lecture Notes in Computer Science, 2008, , 741-748.	1.3	30
370	Sparse Component Analysis: a New Tool for Data Mining. Springer Optimization and Its Applications, 2007, , 91-116.	0.9	23
371	How to extract marker genes from microarray data sets. Annual International Conference of the IEEE Engineering in Medicine and Biology Society, 2007, 2007, 4215-8.	0.5	6
372	Sparse Nonnegative Matrix Factorization with Genetic Algorithms for Microarray Analysis. Neural Networks (IJCNN), International Joint Conference on, 2007, , .	0.0	12
373	Joint low-rank approximation for extracting non-Gaussian subspaces. Signal Processing, 2007, 87, 1890-1903.	3.7	10
374	A bilinear algorithm for sparse representations. Computational Optimization and Applications, 2007, 38, 249-259.	1.6	9
375	Pivot Selection Strategies in Jacobi Joint Block-Diagonalization. Lecture Notes in Computer Science, 2007, , 177-184.	1.3	6
376	A Toolbox for Model-Free Analysis of fMRI Data. Lecture Notes in Computer Science, 2007, , 209-217.	1.3	1
377	Identifiability Conditions and Subspace Clustering in Sparse BSS. , 2007, , 357-364.		2

Blind Matrix Decomposition Techniques to Identify Marker Genes from Microarrays. , 2007, , 649-656.

#	Article	IF	CITATIONS
379	Blind Matrix Decomposition Via Genetic Optimization of Sparseness and Nonnegativity Constraints. Lecture Notes in Computer Science, 2007, , 799-808.	1.3	1
380	Colored Subspace Analysis. , 2007, , 121-128.		1
381	Independent Subspace Analysis Is Unique, Given Irreducibility. , 2007, , 49-56.		6
382	Statistical Analysis of Sample-Size Effects in ICA. , 2007, , 416-425.		1
383	Median-based clustering for underdetermined blind signal processing. IEEE Signal Processing Letters, 2006, 13, 96-99.	3.6	25
384	Robust Sparse Component Analysis Based on a Generalized Hough Transform. Eurasip Journal on Advances in Signal Processing, 2006, 2007, 1.	1.7	7
385	Blind source separation based on self-organizing neural network. Engineering Applications of Artificial Intelligence, 2006, 19, 305-311.	8.1	3
386	On the use of sparse signal decomposition in the analysis of multi-channel surface electromyograms. Signal Processing, 2006, 86, 603-623.	3.7	23
387	On the use of simulated annealing to automatically assign decorrelated components in second-order blind source separation. IEEE Transactions on Biomedical Engineering, 2006, 53, 810-820.	4.2	5
388	Separation of water artifacts in 2D NOESY protein spectra using congruent matrix pencils. Neurocomputing, 2006, 69, 497-522.	5.9	8
389	Denoising using local projective subspace methods. Neurocomputing, 2006, 69, 1485-1501.	5.9	34
390	A Fast Predictive Lossless Coder for fMRI Data Sets. , 2006, , .		0
391	Optimization Algorithms for Sparse Representations and Applications. , 2006, , 85-99.		2
392	Sparse Nonnegative Matrix Factorization Applied to Microarray Data Sets. Lecture Notes in Computer Science, 2006, , 254-261.	1.3	4
393	Estimating Non-Gaussian Subspaces by Characteristic Functions. Lecture Notes in Computer Science, 2006, , 157-164.	1.3	6
394	Extended Sparse Nonnegative Matrix Factorization. Lecture Notes in Computer Science, 2005, , 249-256.	1.3	9
395	On model identifiability in analytic postnonlinear ICA. Neurocomputing, 2005, 64, 223-234.	5.9	5
396	Sparse Component Analysis and Blind Source Separation of Underdetermined Mixtures. IEEE Transactions on Neural Networks, 2005, 16, 992-996.	4.2	280

#	Article	IF	CITATIONS
397	A Fast and Efficient Method for Compressing fMRI Data Sets. Lecture Notes in Computer Science, 2005, , 769-777.	1.3	4
398	3D Spatial Analysis of fMRI Data on a Word Perception Task. Lecture Notes in Computer Science, 2004, , 977-984.	1.3	4
399	Blind source recovery: algorithm comparison and fusion. AIP Conference Proceedings, 2004, , .	0.4	0
400	A New Concept for Separability Problems in Blind Source Separation. Neural Computation, 2004, 16, 1827-1850.	2.2	32
401	Spatial ICA of fMRI data in time windows. AIP Conference Proceedings, 2004, , .	0.4	9
402	A geometric algorithm for overcomplete linear ICA. Neurocomputing, 2004, 56, 381-398.	5.9	89
403	Mobile decision support for transplantation patient data. International Journal of Medical Informatics, 2004, 73, 461-464.	3.3	14
404	Uniqueness of complex and multidimensional independent component analysis. Signal Processing, 2004, 84, 951-956.	3.7	43
405	Blind Source Separation of Linear Mixtures with Singular Matrices. Lecture Notes in Computer Science, 2004, , 121-128.	1.3	5
406	Postnonlinear Overcomplete Blind Source Separation Using Sparse Sources. Lecture Notes in Computer Science, 2004, , 718-725.	1.3	7
407	Second-Order Blind Source Separation Based on Multi-dimensional Autocovariances. Lecture Notes in Computer Science, 2004, , 726-733.	1.3	9
408	Removing water artefacts from 2D protein NMR spectra using GEVD with congruent matrix pencils. , 2003, , .		1
409	Neural network signal analysis in immunology. , 2003, , .		0
410	Mathematics in independent component analysis. , 2003, , .		4
411	Generalizing Geometric ICA to Nonlinear Settings. Lecture Notes in Computer Science, 2003, , 687-694.	1.3	2
412	Linear Geometric ICA: Fundamentals and Algorithms. Neural Computation, 2003, 15, 419-439.	2.2	54
413	Adaptive signal analysis of immunological data. , 2003, , .		0
414	SOMICA and geometric ICA. , 2003, , .		1

#	Article	IF	CITATIONS
415	A new ica method based on a lattice of the observation space. , 2003, , .		1
416	An improved geometric overcomplete blind source separation algorithm. Lecture Notes in Computer Science, 2003, , 265-272.	1.3	0
417	An Adaptive Approach to Blind Source Separation Using a Self-Organzing Map and a Neural Gas. Lecture Notes in Computer Science, 2003, , 695-702.	1.3	0
418	Topological Constructions in the o–Graph Calculus. Mathematische Nachrichten, 2002, 241, 170-186.	0.8	1
419	Comparison of maximum entropy and minimal mutual information in a nonlinear setting. Signal Processing, 2002, 82, 971-980.	3.7	3
420	Overcomplete ICA with a Geometric Algorithm. Lecture Notes in Computer Science, 2002, , 1049-1054.	1.3	4
421	Pattern Repulsion Revisited. Lecture Notes in Computer Science, 2001, , 778-785.	1.3	3
422	Denoising using local ICA and kernel-PCA. , 0, , .		4
423	Postnonlinear blind source separation via linearization identification. , 0, , .		1
424	Clustering of dependent components: a new paradigm for fMRI signal detection. , 0, , .		1
425	Blind Sensor Characteristics Estimation in a Multi-Sensor Network Applied to fMRI Analysis. , 0, , .		0
426	Kernel-PCA denoising of artifact-free protein NMR spectra. , 0, , .		1
427	Blind signal separation into groups of dependent signals using joint block diagonalization. , 0, , .		28
428	An algorithm for automatic assignment of artifact-related independent components in biomedical signal analysis. , 0, , .		0